Strojnícky časopis – *Journal of* MECHANICAL ENGINEERING,
VOL 72 (2022), NO 1, 35 – 48

PREDICTING THE BURNISHING FORCE FOR CYLINDRICAL WORKPIECES WITH AMODIFIED SURFACE LAYER

FANIDI Omar[1*], KOSTRYUKOV Alexandre[2], SHCHEDRIN Alekcie[3]

[1]Ecole Nationale Supérieure d'Arts et Métiers, Hassan II University, Casablanca, Morocco,
e – mail: omarfanidi75@gmail.com
[2]Machine-Building Plant, Demikhovsky, Orekhovo-Zuevo, Russia
[3] MT13, Engineering technology, Bauman Moscow State Technical University, Moscow, Russia

Abstract: A mathematical module for predicting and analysing the drawing forces is formed and verified. The process used in the current study is drawing. Geometric parameters of the deformation zone and the "selective transfer phenomenon" are also taken into consideration. The experimental verification is conducted through two tests: In the first test, the experimental blanks are cylindrical rods (steel 45, length 150 mm), and are preliminary turned, and the drawplate made of steel 9xc, are used. Regular micro-relief (RMR) hardens the working surfaces of the drawplate. In the second test, the same conditions are applied except for the samples, which represent solid cylindrical billets made of steel 45 with a complicatedly modified surface layer, including a brass film, regular microgeometry and a "servo-witte" copper film. As a result, in the first experiment, the discrepancies are in the range of -29.1% up to +23%. In the second experiment, the discrepancies are in the range of +1.38% up to +48.9%.

KEYWORDS: drawing force, regular micro-relief, deformation zone, metal-cladding lubricants.

1 Introduction

Drawing is a highly efficient method for machining, finishing and hardening holes on workpieces with various dimensions, structures and shapes. [1-3].

Applied to solid cylindrical profiles, the current methods of processing are systemically and intensively improved through the use of self-organizing tribotechnologies, which include regularizing microgeometry and surface modification of a drawing tool and workpiece, as well as various methods of influence by metal-clad lubricants which allow to realize the fundamental scientific principle « Garkunov-Kragelsky effect, friction without wear » [4-15]..

This machining method allows to reduce the drawing force by 25 ... 75%, and to increase quality and productivity up to the double. It also allows to form a protective film ("servo-witte") which contributes in a significant reduction in the cost of drawing tools [9-15].

When choosing technological equipment for the implementation of the relevant drawing operations, it is necessary to accurately predict the processing forces [1, 2, 17-21]. At the same time, the most accurate theoretical model for predicting and analysing the drawing forces of solid cylindrical billets is Vorontsov's expression [19], which additionally has a wide physical visibility. In this work, the mathematical module for predicting the drawing forces of continuous cylindrical workpieces is considered and verified. This adaptation has taken into account the deformation zone parameters and the "selective transfer phenomenon". For this reason two experimental studies are applied on two different samples.

DOI: 10.2478/scjme-2022-0004, Print ISSN 0039-2472, On-line ISSN 2450-5471

2 Analytical model

Vorontsov relied on bronze, brass and copper [19] as basic elements in his experiments dedicated to the verification of the theoretical model of the drawing force expression. Another particularity in his experiments is that he focused on the impact which the conical part angle of the deformation element has on the drawing force. The optimal angle is in the interval 5… 9°. However the model proposed by Vorontsov takes into account neither the actual geometry of the deformation zone ΔR_b, nor the properties of metal-clad lubricants, nor the phenomenon of "selective transfer under friction" in the form of a "servo film" h_{sw} [22, 23], nor the roughness parameters χ_b , R_{sw} and $H_{b\,max}$. To eliminate these imperfections and to enrich this study, the experimental and theoretical results obtained previously are used to formulate the mathematical model (1) of the drawing force.

$$\begin{cases} q_d^{\mathrm{T}} = 0.25(D_l - 2h_{sw})\bar{\sigma}_s \left[\left(2 + f\dfrac{sin\alpha}{1-cos\alpha}\right) ln\left(\dfrac{D_b \pm 2\Delta R_b + 2h_{sw}}{D_l - 2h_{sw}}\right) + \dfrac{1-cos\alpha}{sin\alpha} + 2f\dfrac{L_l}{(D_l - 2h_{sw})}\right]; \\ F_d^{\mathrm{T}} = \pi q_d^{\mathrm{T}}(D_l - 2h_{sw}); \\ q_a^{\mathrm{T}} = \dfrac{E(\chi_b + 1)}{\pi K_1 K_2(\chi_b + 1.5)}\sqrt{\dfrac{\varepsilon_b H_{b\,max}}{K_b R_{sw}}}; \\ f = f_a + f_d = \left(\dfrac{\pi K_1 K_2(\chi_b + 1.5)}{E(\chi_b + 1)}\tau_0\sqrt{\dfrac{K_b R_{sw}}{\varepsilon_b H_{bmax}}} + \beta\right) + \left(0.28\sqrt{\dfrac{\varepsilon_b H_{b\,max}}{R_{sw}}}\right); \end{cases} \quad (1)$$

Where:

q_d^{T} - Theoretical specific (linear) drawing force, N/mm,

D_l - Diameter of the working channel of the deforming drawplate in a calibrating ribbon, mm,

h_{sw} - The thickness of the part of the modified layer in the form of a protective film ("servo-witte"), mm,

$\bar{\sigma}_s$ - The average yield stress of the material processed according to (in) the deformation zone, MPa;

f - Sliding friction coefficient;

f_a and f_d - Respectively, the adhesive and the deformation component of the coefficient of sliding friction;

α - The angle of the working cone of the deforming drawplate;

D_b - Diameter of the workpiece before drawing, taking into account the thickness of the additional layer as a result of regularization of the surface microgeometry and the application of an anti-friction coating [11, 12, 15], mm;

ΔR_b - Parameter of the deformation zone in the form of a sign and wave height of non-contact deformation arising on the working cone of the drawplate, mm; (fig.3, fig.4 and fig. 5);

L_l - Width of the calibrating ribbon deforming the drawplate, mm;

F_d^{T} - Theoretical total drawing force, N;

q_a^{T} - Theoretical actual contact pressure on the working cone of the deforming drawplate, MPa;

E - Modulus of elasticity, MPa;

χ_b - Parameter of the law of the altitudinal distribution of micro-speaks of the rough surface of the workpiece before drawing;

K_1, K_2 and K_3 - Coefficients of the general solution of the Hertz-Belyaev contact problem;

R_{sw} - The radius of curvature at the summit of a single micro protrusion of the rough surface of the working channel of the deforming drawplate, μm;

ε_b - Relative deformation of the maximum micro protrusion of the rough surface of the workpiece as a result of drawing;

$H_{b\,max}$ - The height of the maximum micro protrusion of the rough surface of the workpiece for drawing, μm;

τ_0 - Strength adhesive connections at $q_a^{\mathrm{T}} = 0$ MPa;

β - Piezocoefficient influence q_a^{T} on strength adhesive connections.

Hence, the derivation and determination of the above parameters and coefficients are partially considered in [5, 19, 23].

3 Experimental study

3.1. First experimental study

As the first experimental base for testing the theoretical model of the drawing force (1), the process of drawing solid cylindrical billets made of steel 45 (174 ... 187 HB) through a deforming drawplate made of steel 9XC (58… 61 HRC) is considered [10]. In this process, the tool used is similar to that of the works [8, 9, 13, 14]; their working surface is strengthened by the creation of a regular micro-relief in the form of single-turn threaded channels with a radius of 1.5 mm, a pitch of 0.5 mm and an initial depth in the calibration-strip section of 10μm. Tests were carried out at five specimens that have the following diameters: $D_b = 20.091$mm; $D_b = 20.206$ mm; $D_b = 20.295$ mm ; $D_b = 20.389$ mm; $D_b = 20.489$ mm. The actual tension is calculated by the expression $i_a = D_b - D_l$; where $D_l = 20$ mm is diameter over the calibration bland (tool diameter figure 3). Therefore the first specimen is deformed by tension $i_a = 0.091$ mm, the second by $i_a = 0.206$ mm, the third by $i_a = 0.295$ mm, the fourth by $i_a = 0.389$ mm, and the fifth by $i_a = 0.489$ mm. The length of the part that undergoes drawing is 150 mm [10, 13]. Profilometers Maud 201 and Maud 296 are used to obtain the profile-grams. The longitudinal profile-grams of the blanks surface of the before drawing (after turning) used to determine the parameters χ_b and $H_{b\,max}$ are shown in Figure 1, where: Ra_b, - the surface roughness parameter of the sample blanks before drawing.

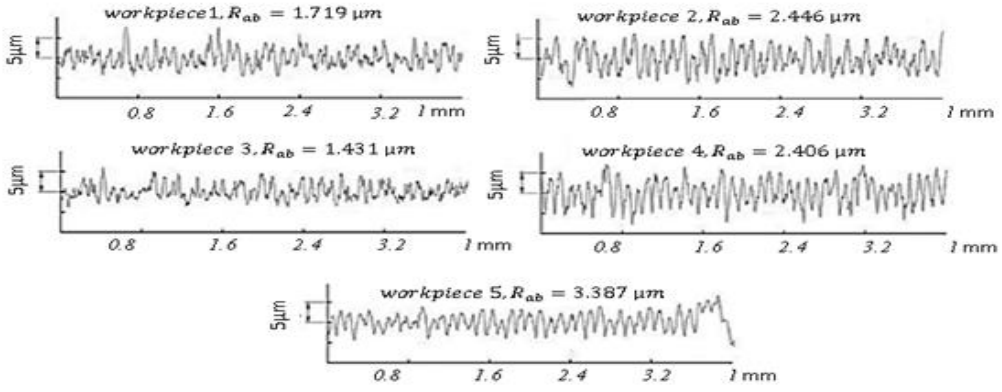

Fig. 1 Longitudinal profile-grams of rough surfaces of blanks made of steel 45. Horizontal increase x20; vertical increase x1000

The longitudinal profile-gram of the calibration-strip in the deforming drawplate [10] for determining the radius R_{sw}, is shown in Figure 2. A diamond tool (radius *1.5* mm) is used to produce regular micro-relief, in the form of single-turn helical channels (groove depth: $D_{ch} =$ 10 μm, groove pitch: $P_{ch} = 0.5$ mm). Here Ra_t is the surface roughness parameter of the working channel of the drawplate according to the calibrating strip (tool).

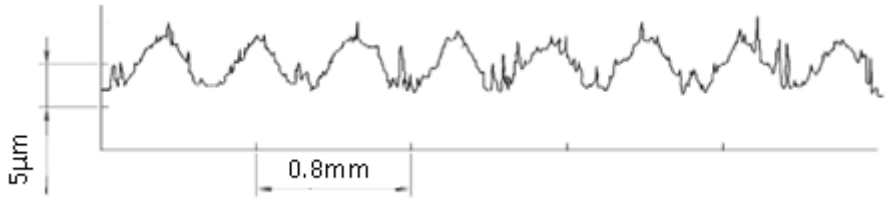

Fig. 2 Longitudinal profile-gram of the calibrating band for deforming drawplate with a regular micro-relief: material 9XC, $Ra_t = 1.791$ μm. Horizontal increase x20; vertical increase x1000

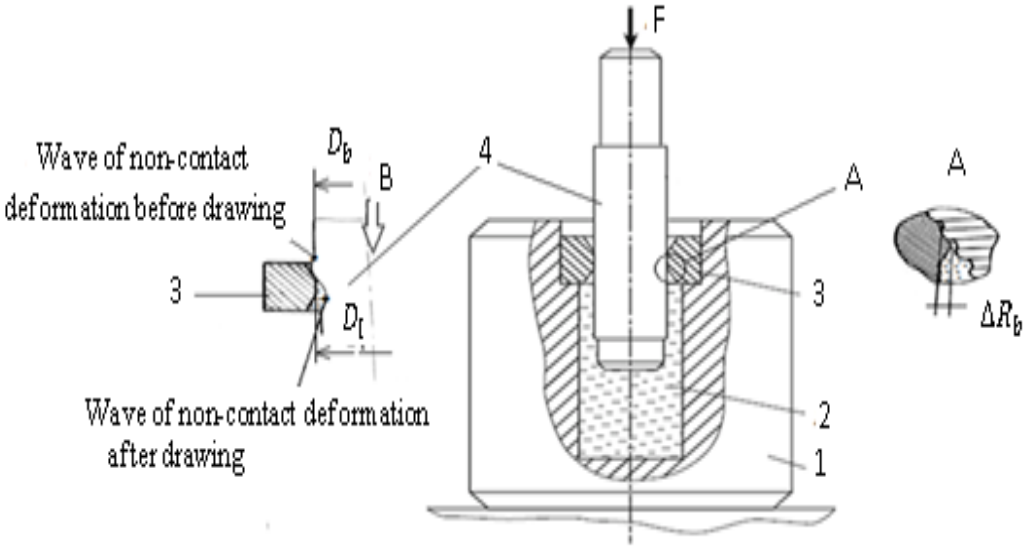

Fig. 3 The experimental setup. A) the parameter ΔR_b, B) the deformation zone.
1- The thin-walled cylinder, 2- Cavity with lubricant, 3- Drawplate (tool), 4- Workpiece.

The drawing speed is *1* m/min. The lubricant employed is *I-40* mineral oil with an admixture of oil-soluble "Valen" metal-coating additive at *50* vol %, realizing the fundamental scientific principle « Garkunov-Kragelsky effect, friction without wear (selective transfer) » [4, 9, 10, 13, 14, 25]. Figure 3 presents the schematic view of experimental setup: a thin walled cylinder 1 with a cavity 2 for lubricant. In the upper part of cylinder 1, there is a machining drawplate 3, whose working surfaces are hardened by a regular micro-relief (fragment A). When blank 4 passes through drawplate 3 into cavity 2, the lubricant pressure attains the required value for flowing in the micro-relief channels on the working surface of drawplate 3. Figure 3 fragment A shows the parameter of the deformation zone (ΔR_b) in the form of a sign and wave height of non-contact deformation arising on the working cone of the drawplate, whereas fragment B shows the deformation zone.

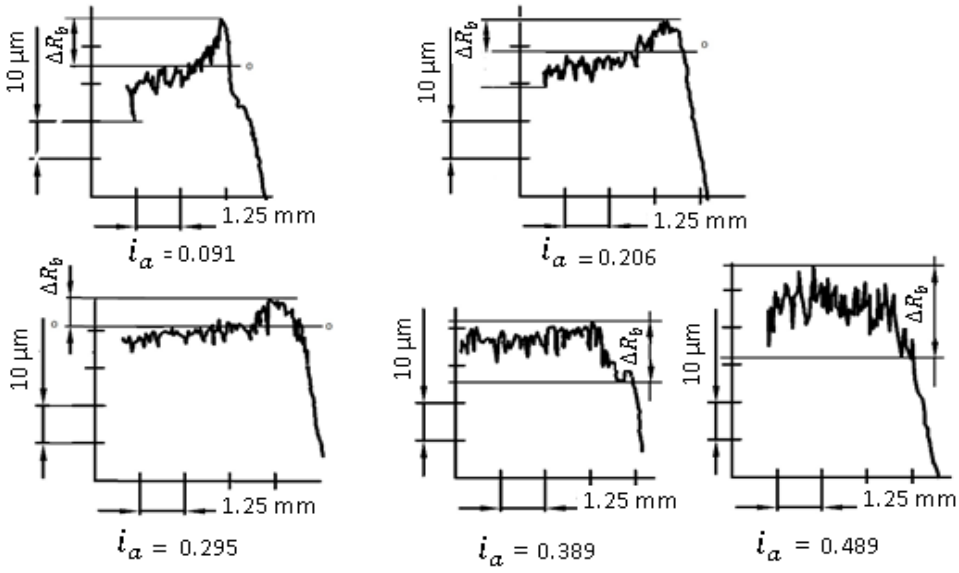

Fig. 4 Longitudinal profile-gram of the deformation zone at the working cone of the deforming drawplate: $D_{ch} = 10$ µm, $P_{ch} = 0.5$ mm; steel 45; lubricant "I-40" + 50% metal-clad additives; horizontal increase x8; vertical increase x1000.

In order to determine ΔR_b (figure 3 fragment A), the profile-gram presented in figure 4 is considered. The analysis of figure 4 shows that a deformation zone is formed on the working cone of the drawplate in the form of a positive wave of non-contact deformation (fragment B) when $i_a > 0.389$ mm and in the form of a negative wave when $i_a < 0.389$ mm. The results obtained by determining the parameter ΔR_b are presented in figure 5.

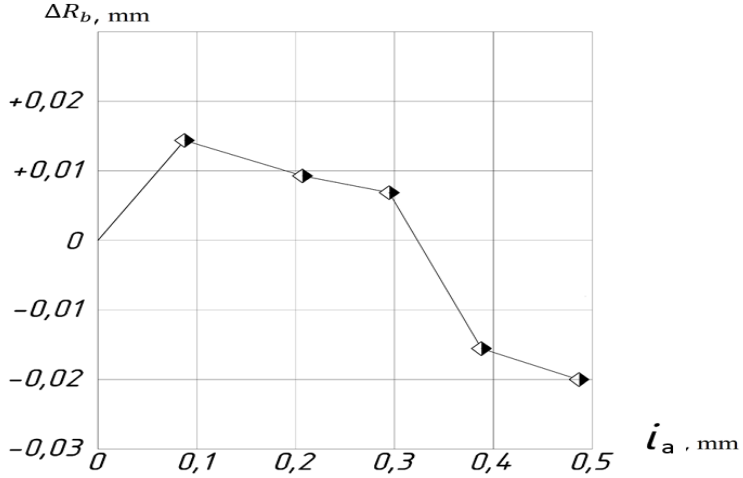

Fig. 5 Dependence of the magnitude and sign of non-contact deformation on the actual absolute deformation: $D_{ch} = 10$ µm, $P_{ch} = 0.5$ mm; steel 45; lubricant "I-40" + 50% metal-plating additives.

For real calculations with the mathematical model (1), the hardening of the material used is tested according to GOST 25.503-97. The resulting hardening curve for steel 45 is shown in Figure 6. Where e_i is the accumulated deformation of the workpiece (the degree of deformation) who is calculated using expression (2):

$$e_i = 2\,ln\left(\frac{D_b + 2\Delta R_b}{D_l}\right) \quad (2)$$

The accumulated deformation is a quantity whose total derivative in time is equal to the intensity of the deformation speed φ_i (3):

$$\varphi_i = \frac{de_i}{dt} \tag{3}$$

The resulting overall hardening curve for steel 45 is shown in Figure 6a. The considered range of the accumulated deformation of the workpiece e_i [19] in the experimental study is in the range $e_i = 0{,}011 \ldots 0{,}044$; Therefore, to obtain the equation of the hardening curve, the results were approximated in the range $e_i = 0{,}00675 \ldots 0{,}045$. The partial hardening curve approximated at this site is shown in Figure 6 b, and the expression for this hardening curve is:

$$\sigma_s = 241.061 + 5872\, e_i \tag{4}$$

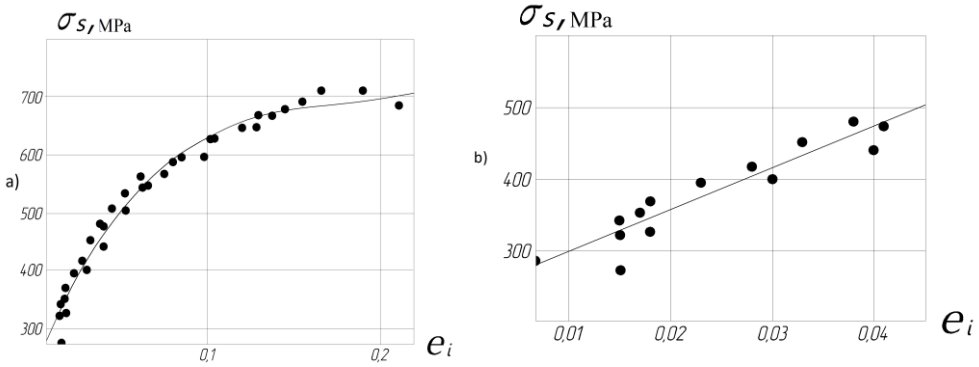

Fig. 6. Hardening curve of steel 45: a) total; b) partial

The initial information and the calculation results by the mathematical model, as well as the comparison of theoretical q_d^{T} and experimental q_d^e specific drawing forces are given in Table 1. In this case, the analytical dependence of the experimental drawing (broaching) specific force has the expression (N / mm):

$$q_d^e = 49.363 + 364.31 i_a \tag{5}$$

After approximation of the results obtained, the analytical dependence of the theoretical drawing (broaching) specific force is (N/mm):

$$q_d^{\mathrm{T}} = 76.279 + 236.34 i_a \tag{6}$$

Figure 7 presents a graphical interpretation of the comparison of both theoretical and experimental dependence of the drawing (broaching) specific force.

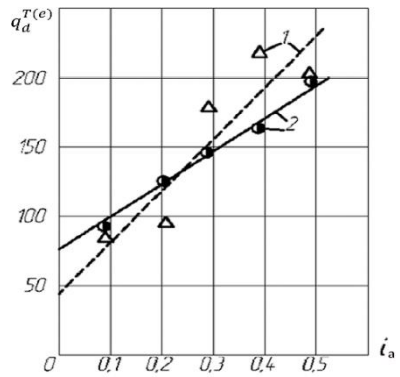

Fig. 7 Dependence of the specific drawing force on the absolute actual strain deformation: 1- experimental; 2- theoretical.

Table 1. Baseline data for the calculation and comparison of the specific drawing force

Parameter	Workpiece				
	1	2	3	4	5
i_a, mm	0.091	0.206	0.295	0.389	0.489
D_b, mm	20.091	20.206	20.295	20.389	20.489
ΔR_b,mm	+0.014	+0.009	+0.007	-0.016	-0.020
$\boldsymbol{\chi_b}$	1.367	0.345	1.132	1.340	1.441
h_{sw}, μm	1.5	1.5	1.5	1.5	1.5
e_i	0.01186	0.02227	0.03066	0.03538	0.0444
$\bar{\sigma}_s$, MPa	275.89	306.46	331.089	344.93	371.4
D_l, mm	20	20	20	20	20
α, grad	5	5	5	5	5
L_l, mm	5	5	5	5	5
$H_{b\,max}$, μm	11.5	13	9.0	15.5	21.0
ε_b	0.896	0.920	0.917	0.940	0.953
R_{cs} , μm	8727	8727	8727	8727	8727
K_1	3.778	3.778	3.778	3.778	3.778
K_2	0.408	0.408	0.408	0.408	0.408
K_3	1.220	1.220	1.220	1.220	1.220
τ_0 , MPa	9.873	9.873	9.873	9.873	9.873
β	0	0	0	0	0
f	0.016	0.017	0.016	0.016	0.017
q_d^e, N/mm	85.8	95.96	*178.37*	217.89	204.34
q_d^{T}, N/mm	93.65	123.9	148.93	167.7	198.82
Δq_d, %	-9.14	-29.1	+16.5	+23	+2.7
q_a^{T}, MPa	1595	1517.7	1400.8	1893.3	2235

To estimate the theoretical contact pressure q_a^{T} on the working cone of the deforming element, the following dependences are used:

$$L_a = \frac{0.5 i_a + \Delta R_b}{sin\alpha} \tag{7}$$

$$D_c = 0.5(2D_l - (i_a + 2\Delta R_b) \tag{8}$$

According to the data in Table 1, the theoretical actual contact pressure q_a^{T} has a maximum value when $i_a \geq 0.389$.

This regularity is explained by the fact that with an increase in the degree of deformation i_a, the actual contact width grows faster than theoretical total drawing force F_d^{T} and vice versa.

3.2. Second experimental study

As a second experimental basis for verifying the reliability of the theoretical model of the drawing force (1), a process similar to the above-mentioned one is considered. However, the second considered process slightly differs from the first one in terms of the used samples which represent solid cylindrical billets made of steel 45 (186 HB) with a complicatedly modified surface layer; including a brass layer, a regular microgeometry (Fig. 8) and a "servo-witte" copper layer [12]. These modifications resulted in a wave absence in deformation zone (Fig. 9) [11, 15]. Tests were carried out at five specimens that have the following diameters: $D_b = 20.133$ mm, $D_b = 20.246$ mm, $D_b = 20.335$ mm, $D_b = 20.453$ mm and $D_b = 20.560$ mm. The actual tension is calculated by the expression $i_a = D_b - D_l$; where $D_l = 20$ mm is diameter over the calibration bland (tool diameter figure 3). Therefore the first specimen is deformed by tension $i_a = 0.133$ mm, the second by $i_a = 0.246$ mm, the third by $i_a = 0.335$ mm, the fourth by $i_a = 0.453$ mm, and the fifth by $i_a = 0.56$ mm. The length of the part that undergoes drawing is 150 mm [10, 13].

The initial data for the calculation and comparison of the theoretical drawing specific force are given in Table 2.

In this case, the hardening curve, taking into account the preliminary plastic deformation and regularization of the surface microgeometry of the blanks [11, 12, 15] (the depth of the grooves of 20 μm) (Fig. 8.9), takes the expression (MPa):

$$\sigma_s = 264 + 5872e_i \tag{9}$$

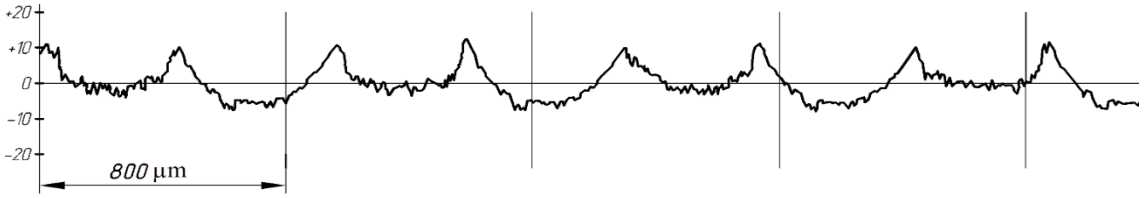

Fig. 8 Longitudinal profilogram of the surface of a cylindrical billet of steel 45 with a regular microgeometry of the surface in the form of one-way helical grooves with a radius of 1.5 mm, a step of 1 mm and a depth of grooves of 20 μm. Horizontal increase x75; vertical increase x1000

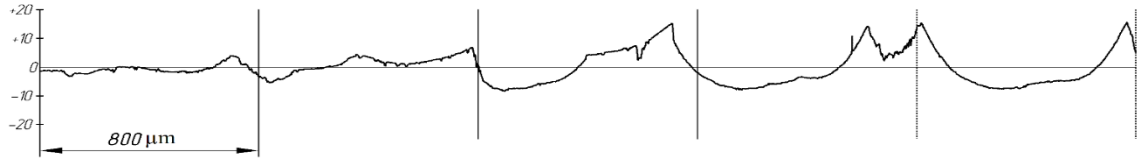

Fig. 9 Longitudinal profilogram of the deformation zone arising on the working cone of the deforming drawplate when drawing a solid cylindrical billet with a difficult modified surface layer: $i_a = 0.56$ mm; the depth of the grooves of the regular microrelief 20 μm; thickness of the brass-coated layer is 5 μm; grease I-40 + 50% metal-clad additives. Horizontal increase x75; vertical increase x1000

Therefore, the coefficient of sliding friction is determined by the expression [5]:

$$f = f_a + f_d = \left(\frac{\tau_0}{HB_b} + \beta\right) + \left(0.28\sqrt{\frac{\varepsilon_b H_{bmax}}{R_{cs}}}\right) \quad (10)$$

where $HB_b -$ surface hardness, MPa;

R_{cs} - The reduced radius of curvature at the summit of single micro-protrusions of the rough surfaces of the workpiece and the working channel of the deforming drawplate, μm.

The reduced radius of curvature at the summit of single micro-protrusions of the rough surfaces R_{cs} is obtained by the expression (11) given in the work [26].

$$R_{cs} = \frac{4}{\frac{1}{R_{b_x}} + \frac{1}{R_{b_y}} + \frac{1}{R_{t_x}} - \frac{1}{R_{t_y}}} \quad (11)$$

Where $R_{b_x}, R_{b_y}, R_{t_x}, R_{t_y}$ - respectively represent, the longitudinal (x) and transverse (y) radius at the summit of single micro-protrusions of the workpiece rough surfaces (b) as well as the working channel of the deforming drawplate (t) in μm.

After approximation of the experimental and theoretical specific force values, the analytical dependencies are obtained as follows: (N/mm):

$$q_d^e = 214.826 + 290.843\ i_a \quad (12)$$

$$q_d^{\mathrm{T}} = 67.11 + 533.65\ i_a \quad (13)$$

The analysis of expressions (12) and (13) shows that they converge at $i_a = 0{,}608$ mm. Figure 10 presents a graphical interpretation of the comparison of both the theoretical and the experimental dependence of the drawing (broaching) specific force.

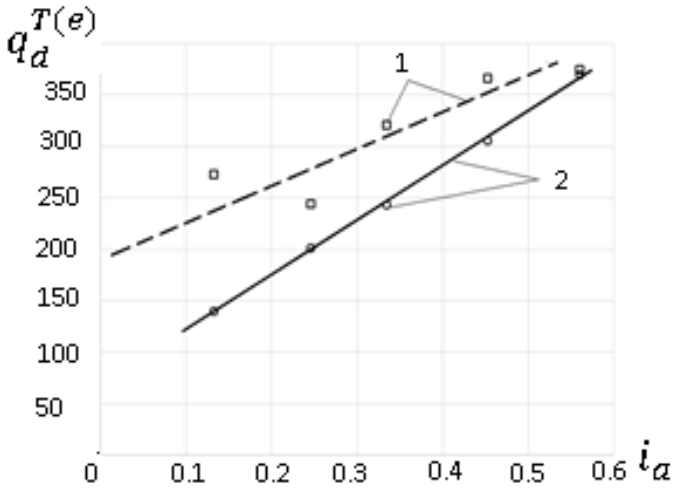

Fig. 10 Dependence of the specific drawing force on the absolute actual strain deformation: 1- experimental; 2- theoretical.

To conclude, we notice that in the deformation zone, the wave in non-contact deformations is absent. This leads automatically to the absence of the actual contact width of the working cone of the deforming element with the workpieces. Thus, there is the contact pressure is practically absent on the working cone.

DISCUSSION

The analysis of the results (Table 1) shows that in the range $i_a = 0{,}091 \ldots 0{,}489$ mm, the relative percentage error of the theoretical values of the drawing specific force ($\Delta q_d = \left(\frac{q_d^e - q_d^{\mathrm{T}}}{q_d^e}\right) 100\%$) ranges from - *29.1 to + 23% ;* whereas, the experimental dependence (5) and the theoretical dependence (6) converge when $i_a = 0{,}21$ mm (Fig. 7). This is due to the wide spread in the roughness parameters of the surface of the workpieces before drawing (Fig. 1, table 1); which significantly affects the mechanisms involved in a tribological contact in accordance with the applied formulas of the coefficient of sliding friction $f = f_a + f_d$ in expression (1) and the actual contact pressure q_a^{T}.

This actual contact pressure significantly exceeds the average yield stress of the processed material $(q_a^{\mathrm{T}} \gg \bar{\sigma}_s)$ at the deformation center, which indicates a similar ratio of the actual and nominal contact areas between the workpiece rough surfaces and the tool's ones (i.e. working channel of the deforming drawplate) (Fig. 1, 2) [4, 5]. Contact pressure exceeds the average yield stress that leads to the stimulation of the stresses in the workpiece; hence, resulting in deep micro-cracks; which, in their turn, pass into the finished product's surface layer and reduce its performance.

The use of metal lubricants, tools and workpieces with a regular micro-relief has proved to be very efficient, as it has allowed a significant reduction in friction and deformation energy costs as well as contributing in a complete elimination of the adhesion of the processed material.

While using the samples with an irregular micro-relief (Fig. 1), a positive wave of non-contact deformation arises on the drawplate's working cone, which increases the contact area between the tool surface and the workpiece surface, and then making it difficult for the lubricant to get into the deformation zone. As a consequence the realization of the hydrodynamic lubrication regime is disrupted, hence leading to an increase in the processing force.

The wave of non-contact deformation causes the tensile stresses and the formation of cracks passing into the surface layer. This leads to low product life, poor metallurgical properties and overall poor product quality.

When using the samples with a regular micro-relief (Fig. 8), the material, being thrust by the drawplate, fills in each groove of the regular micro-relief, thus causing a complete absence of the non-contact deformation negative/positive wave on the active cone of the tool (drawplate's working cone) (fig. 9) [11, 15].

The effect of "the regular micro-relief grooves" on the specimen surface may be explained by the violation of the deformable layer continuity.

Table 2 Baseline data for the calculation and comparison of the theoretical specific drawing force of solid

Parameters	Workpieces				
	1	2	3	4	5
i_a, mm	0.133	0.246	0.335	0.453	0.56
D_b, mm	20.133	20.246	20.335	20.453	20.560
$H_{b\,max}$, μm	28.37	28.833	28.833	28.832	28.82
ε_b	0.5169	0.963	0.959	0.9518	0.95
e_i	0.01325	0.0244	0.0332	0.04479	0.0552
$\bar{\sigma}_s$, MPa	291.64	324.5	350.2	384.09	414.66
ΔR_b, mm	0	0	0	0	0
B	0	0	0	0	0
τ_0 , MPa	42.965	42.965	42.965	42.965	42.965
HB_b, MPa	1860	1860	1860	1860	1860
R_{t_x}, μm	3125	3125	3125	3125	3125
R_{t_y}, μm	10000	10000	10000	10000	10000
R_{b_x}, μm	273	273	273	273	273
R_{b_y}, μm	10065	10123	10167	10226	10280
R_{cs} , μm	1007	1007	1007	1007	1007
f_a	0.023	0.023	0.023	0.023	0.023
f_d	0.03378	0.04649	0.04639	0.04622	0.0461
F	0.05678	0.06949	0.06939	0.0692	0.0691
D_l, mm	20	20	20	20	20
α, grad	5	5	5	5	5
L_l, mm	5	5	5	5	5
q_d^{T}, MPa	139.156	200.44	243.24	305.38	369
q_d^e, N/mm	272.29	243.63	320.06	366.24	374.2
Δq_d, %	+48.9	+17.7	+24	+16.6	+1.38

CONCLUSION

Based on the review of literature and the experiments that have been carried out, some conclusions are deduced:

- A mathematical module to predict the drawing forces of continuous cylindrical parts is formed and verified. The consideration is made to take into account the geometrical parameters of the deformation zone and the "selective transfer phenomenon". For the verification, two identical experiments are conducted. In the

first experiment, the samples are machining by turning. But in the second experiment, the specimens are distinguished by the superficial layer, which is modified, by a brass-coated layer, a regular microgeometry and a copper layer. As a result, in the first experiment, the differences between theoretical and experimental force values are in the range of -29.1% to + 23% whereas in the second experiment, the differences are in the range of + 1.38% to + 48.9%.

- According to the experimental and analytical results, the maximum force ($q_d^{\mathrm{T}} = 369$ N/mm and $q_d^e = 374.2$ N/mm with $\Delta q_d = +1.38\%$) is obtained when there is no wave of non-contact in the deformation zone and at $i_a = 0.56$ mm.
- The regular micro-relief has a positive effect on the utilization of both the final part and the machining of the blank part.
- The regular micro-relief also increases the precision of the part in terms of noncircular deformation and distortion of the longitudinal cross section.

Furthermore, the results will expand the database for systematic parametric synthesis of new hybrid machining methods. All in all, this research confirms that various combined machining methods may be fundamentally improved by employing Garkunov-Kragelsky wear- free conditions.

REFERENCES

[1] Masters, V.A., Berkovsky, V.S. ”The theory of plastic deformation and pressure treatment of metals”, Moscow, Metallurgy, **1989**. (in Russian)

[2] Zaides, S. A., Emelyanov, V. N., Popov, M. E., “Deforming machining of shafts: monograph”, Irkutsk, ISTU publishing house, **2013**. (in Russian)

[3] Trofimov, V. N. “Improving the technology of drawing of long axisymmetric composite electric conductors”, PhD thesis, Institute of Economics and Economics (branch) of Izhevsk State Technical University, Glazov, **2015**. (in Russian)

[4] Garkanov. D. N., Melnikov, E. L., Babele, V., G. “Tribology based on self-organization”, Lambert Academic Publishing, **2015**. (in Russian)

[5] Shchedrin, A. V., Ulyanov, V. V., Bekaev, A. A., Skoromnov, V. M., Vanyushkina, M. S., Abramova, T. G., Khomyakova N.,V., Chikhacheva N. Yu. “Tribological Principles in the Systematic Design of Competitive Technological Equipment”, Repair, restoration, modernization 4, pp. 15 – 20, **2009**.(in Russian)

[6] Shchedrin, A. V., Kostryukov, A. A., Chihachova, N. Yu. “Artificial technological intelligence as the ideological basis of the generalized system of materials processing methods”, Strengthening technologies and coatings 6, pp. 20 – 26, **2015**. (in Russian)

[7] Yaroslavtsev, V. M. “Development and practical implementation of methodology of search of new methods of material processing”, Bulletin of the Moscow State Technical University, N.E. Bauman, Series Mechanical Engineering 2, pp. 56 – 70, **2007**.(in Russian)

[8] Dzyura, V., Maruschak, P., Tkachenko, I., Kuchvara, I. “Ensuring a Stable Relative Area of Burnishing of Partially Regular Microrelief Formed on End Surfaces of Rotary Bodies”, Strojnícky časopis – Journal of Mechanical Engineering 71 (1), pp.41 – 50, **2021**. DOI: 10.2478/scjme-2021-0004

[9] Shchedrin, A. V., Gavrilov, S. A., Erokhin, V. V., Yerokhin, V. V., Biryukov, A. I., Yushin, D. I. “Improving quality and productivity of methods combined machining by

tools with regular surface microgeometry using metal-cladding lubricants", Uprochnyayushchie Tekhnol. Pokrytiya 8, pp. 21 – 25, **2011**. (in Russian)

[10] Gavrilov S. A. "Improvement of surface plastic deformation process using metal-cladding lubricants", Friction and lubrication in machines and mechanisms 4, pp. 33 – 39, **2013**. (in Russian)

[11] Shchedrin, A. V., Kozlov A. Yu., Kostryukov, A. A. "Improvement of the covering surface plastic deformation due to the regularization of microgeometry of the surface of the workpiece", Strengthening technologies and coatings 13 (4), pp. 162 – 168, **2017**. (in Russian)

[12] Shchedrin, A. V., Kostryukov, A. A. "Application of tribotechnology based on self-organization for the systematic improvement of the processes of cold plastic deformation", Strengthening technologies and coatings 13 (11), pp. 495 – 499, **2017**. (in Russian)

[13] Šofer, M., Fajkoš, R., Halama, R. "Influence of Induction Hardening on Wear Resistance in Case of Rolling Contact", Strojnícky časopis – Journal of Mechanical Engineering 66 (1), pp. 17 – 26, **2016**. DOI: 10.1515/scjme-2016-0007

[14] Shchedrin, A. V., Kozlov, A. Yu. "Improving the use of technology metalplating lubricants covering methods of surface plastic deformation tool with regular microgeometry", Strengthening technologies and coatings 3, pp. 8 – 12, **2014**. (in Russian)

[15] Shchedrin, A. V., Kostryukov, A. A., Mel'nikov, E. L., Lavrinenko, V. Yu., Aleshin, V. F., Chikhacheva, N. Yu. "Perfection of covering surface plastic deformation of billets from aluminum alloys", Strengthening technologies and coatings 14 (7), pp. 291 – 296, **2018**. (in Russian)

[16] Melnikov, E .L., Shchedrin, A. V., Kostryukov, A. A., Seryozhkin, M. A., Stupnikov, V. P., Stupnikov V. V., Patent No. 2647057, Russian Federation, IPC B24B39/00, "Method of cold plastic deformation of metals", Applicant and patent of MGTU named after N.E. Bauman. Stated 05/30/2017. Published 03/13/**2018**. Bul.No.8. (in Russian)

[17] Kucheryaev, B. V., Nikolaev, R. A., Zhukova, E. A. "Calculation of energy parameters of the process of drawing rods", Publishing House "Nauka & Technology", Proizvodstvo Prokata (Rolled Products Manufacturing) 6, pp. 30 – 33, **2006**. (in Russian)

[18] Abramov, A. N., Semenov, V. I., Shuster, L. Sh. "Mathematical modeling of the process of drawing", Forging and stamping production, metal forming 9, pp. 33 – 36, **2003**. (in Russian)

[19] Osadchy, V. Ya., Vorontsov, A. L. "Formula to calculating the drawing stress of round solid profiles", Publishing House "Nauka & Technology", Proizvodstvo Prokata (Rolled Products Manufacturing) 6, pp. 3 – 8, **2001**. (in Russian)

[20] Guryanov, G. N. "Reserves of energy saving during cold drawing of steel wire", http://www.imet.ru/STAL, Stal 12, pp. 53 – 54. **2009**. (in Russian)

[21] Deordiev, N. T., Korobkin, V. D., Chudakov, P. D. "Plastic flow of hardening material in a conical matrix", Forging and stamping production, metal forming 1, pp. 8 – 10, **1970**. (in Russian)

[22] Shchedrin, A. V., Gavrilov, S. A., Kosarev, I. V., Smolkina, T. V., Zinin, M. A., Sergeev, E. S. "Formation of foci of deformation in the surrounding surface plastic deformation", Friction and lubrication in machines and mechanisms 10, pp. 3 – 7, **2014**. (in Russian)

[23] Kuznetsov, V. A., Schedrin, A. V., Gavrilov, S. A., Voronkov, V. I., Mel'nikov, E. L. “Theoretical and experimental researches of encompassing superficial plastic deformation method in conditions of using of metal-cladding lubricants”, Strengthening technologies and coatings 2, pp. 11 – 17, **2014**. (in Russian)

[24] “Metal-containing oil-soluble composition for lubricant materials”, patent for an invention, https://patents.google.com/patent/RU2277579C1/en

[25] Lidorenko, N. S. “Scientific discovery”, Association of the authors of scientific discoveries of the USSR 41, Reg. 21, Diploma No. 41, Moscow, **1996**. (in Russian)

[26] Chebda, M., Chichinadze, A. V. “Handbook of tribotechnology. Lubricants, lubrication technology, sliding and rolling bearings”, "Engineering ", vol. 2, Moscow, **1990**. (in Russian)